1968

The kinetics of Mn0 reduction from Ca0-Al203-Si0z slag by carbon-saturated iron

David M. Koncsics
Lehigh University

THE KINETICS OF MnO REDUCTION FROM $CaO-Al_2O_3-SiO_2$ SLAG BY CARBON-SATURATED IRON

by

David Mathias Koncsics

A Thesis

Presented to the Graduate Committee

of Lehigh University

in candicacy for the Degree of

Master of Science

in

Metallurgy and Material Science

Lehigh University

1968

CERTIFICATE OF APPROVAL

This thesis is accepted and approved in partial fulfillment of the requirements for the degree of Master of Science.

May 20, 1968
(date)

Stephen K. Sarby
Professor in Charge

H. F. Kibbel
Head of the Department

ACKNOWLEDGEMENTS

I would like the extend my thanks to all those who have helped me in carrying out this research program and preparing this thesis. I am especially indebted to the following:

To Dr. S. K. Tarby, my thesis advisor, for his encouragement and advice.

To D. G. Boltz and W. C. Henderson for writing the computer programs.

To F. H. Ruch and his laboratory technicians for analyzing the samples.

To F. J. Kelly, R. Jensen and their shop crew for fabricating the experimental equipment.

To R. A. Schultz for typing the thesis.

To the Bethlehem Steel Corporation for financial support of my graduate studies and this research project.

To my wife Jean who has been patient and understanding throughout the course of study.

To Debbie, Buzzy and Tami who spent many hours waiting patiently for Daddy to finish his homework.

TABLE OF CONTENTS

LIST OF TABLES

LIST OF FIGURES

NOMENCLATURE

A	Interfacial area, cm^2
C_i	Concentration of component i, weight percent
D_i	Diffusion coefficient of component i, cm^2/sec
ΔF^o	Standard free energy of reaction
J_i	Molar flux of component i, $moles/cm^2 \cdot sec$
K_1, K_2, K_3, K_{eq}	Equilibrium constants
MW	Molecular weight
P	Pressure, atmospheres
Q	Slag-metal ratio defined by $\frac{W_M \ MW_{MnO}}{W_S \ MW_{Mn}}$
R	Gas constant, 1.987 cal/mole-^oK
T	Temperature, ^oK unless stated otherwise
V	Volume, cm^3
W	Weight, grams
X_i	Mole fraction of component i
a_i	Thermodynamic activity of component i
b	As subscript, concentration in bulk phase
$\epsilon_i^{(j)}$	Interaction coefficients $\equiv \frac{d\ (\ln \gamma_i)}{d\ (X_j)}$
$e_i^{(j)}$	Interaction coefficients $\equiv \frac{d\ (\log f_i)}{d\ (\%_j)}$
f_i	Henrian activity coefficient of component i

g	As subscript, indicates component is a gas
h_i	Mass-transfer coefficient of component i, cm/sec
i	As subscript to a chemical symbol, concentration at interface
k	Reaction rate constant, min^{-1}
log	Logarithm to the base 10
ln	Natural logarithm
m	As subscript, metal phase
s	As subscript, slag phase
t	Time in seconds unless otherwise indicated
γ_i	Activity coefficient of component i
δ	Effective thickness of the concentration boundary layer, cm
ρ	Fluid density, gm/cm^3
%	Concentration in weight percent
o	As a superscript, conditions at time of initial sample
1,2---n	As a superscript, conditions at the time of sample n+1
f	As a superscript, conditions at the time of final sample
y	Direction of diffusion

ABSTRACT

The rate of the reduction reaction

$$(MnO) + \underline{C}_{sat.} = \underline{Mn} + CO\ (g) \qquad (1)$$

was studied to determine the rate-controlling mechanism. The experiments were conducted in a graphite crucible heated in a vertical induction tube furnace under a carbon monoxide atmosphere. Mathematical analysis of the time-concentration data showed that the reaction occurs in two stages. In the first stage the reaction rate is limited by the transport of oxygen in the metal phase. In the second stage the reaction is chemically controlled and first order reversible. The effect of temperature on the rate of reaction in stage one vs. stage two completely supports the results obtained from the mathematical analysis. An increase in temperature increased the rate of reaction in the chemically controlled second stage. In contrast, in stage one (diffusion controlled) an increase in temperature had no effect on the rate of reaction. An increase in CO bubbling rate increased the rate of reaction in both stages. Bubbling was found to have a greater affect on the reaction rate in stage two. This inconsistency with respect to the mathematical analysis experienced in reaction rate behavior at different CO bubbling rates is qualitatively explained by observations made on a water model of the system.

INTRODUCTION

Pyrometallurgical processes through chemical reaction convert raw materials into products useful to mankind. In today's age of technology it is impossible to name a single commodity whose existence does not in some manner depend upon a product produced by such a process. The reaction vessel design and operating practice necessary to achieve maximum efficiency and production for a given process is dictated by the thermodynamics and kinetics of the system. Thermodynamics determine whether the desired conversion is possible and, if so, the minimum temperature and heat necessary to carry out the conversion. The kinetics of the process defines the rate at which the desired product can be obtained.

The thermodynamics of most reactions encountered in pyrometallurgical processes have been studied and documented to a useful degree. In contrast, relatively little is known about the mechanisms that control the rate of these processes. The purpose of this investigation is to study the rate of manganese oxide reduction from $CaO-Al_2O_3-SiO_2$ slag by carbon-saturated iron and to determine the rate limiting mechanism for the reaction. Once the rate-limiting mechanism has been identified, commercial processes in which the reaction studied has a role could be optimized to achieve maximum MnO reduction rates. Furthermore, it is hoped that the results of this study will contribute to the basic understanding of the kinetics of heterogeneous reactions.

REVIEW OF LITERATURE

The thermodynamics of most heterogeneous reactions encountered in iron and steelmaking processes have been extensively investigated. In contrast, relatively little work has been done on the kinetics of these reactions. Two reasons for this are the complexities of the systems, which in many cases have not been completely defined, and the materials problem encountered in trying to hold molten metal and an oxide slag in a laboratory crucible (other than graphite) at steelmaking temperatures long enough to study the reaction rate. Because of the aforementioned difficulties, to date, kinetic studies have been essentially limited to the investigation of reactions in which one of the phases is carbon-saturated iron (i.e., iron held in a graphite crucible).

The majority of kinetic studies reported in the literature deal with the rate and mechanism of sulfur transfer between iron and slag. One of the earliest investigations of this system by Chang and Goldman[1] showed that the rate of desulfurization is increased by increasing the basicity of the slag. Other investigators[2,3,4] studied the effect of alloying elements on the rate of desulfurization. Results from these latter studies showed that those elements (e.g., silicon and manganese) which normally enhance desulfurization, actually hindered the reaction when their concentrations in the slag phase were excessive. These observations led to the hypothesis that the rate is controlled by two opposing first-order chemical reactions.

The results of an investigation by Schulz[5] supported this theory. With the aid of silicon equilibrium data, Ramachandran, King, and Grant[6,7] have measured the rate of sulfur transfer and the quantity of carbon monoxide evolved under conditions of minimum interference from side reactions. These authors concluded that the reaction is electrochemical in nature. Chipman and Fulton[8] found that when equilibrium is maintained between silicon in the metal and silica in the slag, desulfurization is diffusion controlled. Omission of silicon from the charge caused a drastic slowing of the reaction, indicating the overriding importance of chemical factors in determining the rate of transfer.

A second fundamental reaction which has received some attention has been the reduction of oxides from liquid slags by carbon-saturated iron. Dancy[9] investigated the reduction of pure liquid FeO and pure liquid Fe_3O_4 by carbon-saturated iron. The results indicated that FeO reduction was a first order reaction up to 80 percent reduction. Over the initial 30 percent reduction, which occurred in about 1 to 2 seconds, the magnetite reaction was also interpreted as a first order reaction. Philbrook and Kirkbride[10] studied the reduction of FeO from a lime-alumina slag by carbon-saturated iron and solid graphite. Using the differential method of data analysis, they found the reaction rate for both reactions was second order. The difference between the observed second order relation and the molecularity of the reactions suggests the rate determining step for these reactions may be diffusion controlled. Tarby and Philbrook[11] in studying the rate of FeO

and MnO reduction from silicate and aluminate slags conclude that in both cases reduction takes place in two stages. In the first stage the stirring caused by CO evolution results in forced convection conditions in the slag. The second stage is defined by natural convection conditions in the slag which resulted from the reduction in CO evolution as the rate of reaction subsides. For both reactions, the rate-controlling step was interpreted to be the mass transfer of neutral oxides from the slag to the slag-metal interface.

McCoy and Philbrook[12] studied the reduction of a chromium oxide by carbon-saturated iron. A rotating crucible, which maintained the slag in a whirlpool of iron, and thus prevented reduction by solid graphite, was used. The reaction was found to be chemically controlled and first order with respect to the chromium concentration in the slag.

Chipman and Fulton[13] investigated the reduction of silica from slag by carbon-saturated iron. They found that metal composition and mechanical stirring had little effect on the reaction rate. Due to the slow reaction rate and high energy of activation for the system, it was concluded the reaction is controlled by the breaking of the silicon-oxygen bond. Rawling and Elliott[14] found the rate limiting step for this reaction is the transport of oxygen in the metal phase. Turkdogan, Grieveson, and Beisler[15] had also concluded diffusion of oxygen in the metal is the rate limiting step, but only in the absence of carbon monoxide bubbles at the slag-metal interface. When carbon monoxide bubbles are present at the

interface, the reaction rate is chemically controlled.

Daines[16] studied the reduction of manganese oxide by silicon (zirconia crucibles were employed) and the reduction of manganese oxide by carbon-saturated iron. For reduction by silicon, Daines concludes the reaction is diffusion controlled because the rate of mechanical stirring had a marked effect on the reaction rate, and the effect of temperature was negligible. The effect of other variables identified diffusion of manganese in the iron phase as the slow step. Daines found the rate of reduction of manganese by carbon was quite sensitive to temperature, but unaffected by mechanical stirring. He concludes the rate-controlling step is an interfacial chemical reaction.

EXPERIMENTAL PROCEDURE

A. Apparatus

The induction furnace tube assembly used for this kinetic study is shown schematically in Figure 1. Power was supplied by a 10,000 cycle, 30 KVA, Ajax Magnethermic model MPG-30 motor-generator set. Melt temperatures were measured with a platinum/platinum-10% rhodium thermocouple inserted into the reaction crucible as shown in Figure 1. The thermocouple was calibrated in a Leeds and Northrup model 9004 thermocouple calibrating furnace at 1450°F and 1850°F. The thermocouple readings which were measured with a Leeds and Northrup Type K-3 Universal Guarded Potentiometer were 3°F high at the two temperatures. It was assumed the thermocouple's deviation at higher temperatures was constant and 3°F. Periodic checks of the calibration curve showed that an accuracy to within two degrees fahrenheit was maintained. The furnace temperature was controlled manually, generally, within $\pm$5°C of the desired temperature.

A carbon monoxide atmosphere was maintained in the furnace throughout the run. A diagram of the gas system is shown in Figure 2. CP grade carbon monoxide (99.5 percent min.) was passed through columns of Ascarite and Drierite to eliminate traces of CO_2 and H_2O before the gas entered the furnace. Gas flow rates to the furnace and the graphite bubbler rod were controlled by Fischer Porter flowrators. Flow to the furnace was 2700 cc per minute; this is approximately equivalent to flushing the volume of the furnace assembly once per minute.

The gas bubbler rods were high purity graphite, 8" long with a 1/2" OD and a 1/8" ID. The bubblers were connected to a standard 1/8" pipe which extended up through the brass top plate. Gas discharged into the bath via a 1/8" horizontal passage located 1/2" above the end of the rod.

Graphite crucibles were machined from 2-9/16" and 3-5/8" diameter high purity graphite rods. The internal configurations and dimensions of the two types of crucibles employed in this study are shown schematically in Figure 3.

B. Materials

High-purity materials were used as components for the slag and metal phases. The source of these materials and the quoted purity of each are summarized in Table I.

The slag components were prefused in a graphite crucible, cast into a clean ingot mold, crushed in a jaw crusher, commutated to -20 mesh in an alumina ball mill (Al_2O_3 pickup was negligible), and then magnetically cleaned. The chemical analysis of the two slags used in this study are also listed in Table I. On trials conducted with Slag No. 1, MnO_2 was blended with the slag before it was added to the crucible. In contrast, in Slag No. 2 the MnO was added to the slag as $MnCO_3$ during the prefusion process.

C. Typical Operating Procedure

On a standard run, 190 grams of electrolytic iron and 7 grams of graphite (added to minimize dissolution of the crucible) were charged in the crucible. The charge was slowly heated to the desired temperature (1500°C or 1575°C) in the CO atmosphere. About 10 minutes after the desired

temperature was reached, the CO bubbler was submerged and a mixture containing 95 grams of prefused slag (Slag No. 1) and 7 grams of MnO_2 was added to the crucible through the sampling port with a funnel. Immediately the power input was increased to counteract the chilling effect of the cold addition. Using this procedure, the temperature was under control by the time the first slag sample was taken 5 minutes later.

Slag samples were taken at five minute intervals for one hour by freezing a slag button on a 5/16" diameter copper rod. The sampling port when not in use was sealed by an O-ring plug.

At the end of the run the metal was poured into a mold. The resultant casting was analyzed for silicon and manganese.

D. Chemical Analysis of Samples

The samples were analyzed by the Analytical Section of the Homer Research Laboratories, Bethlehem Steel Corporation, Bethlehem, Pennsylvania.

Silicon was analyzed by the perchloric dehydration gravimetric method. Manganese concentrations were determined by persulfate arsenite titration. Complete slag analysis was obtained spectrographically.

In preparation for chemical analysis, the slag samples were crushed to -No. 100 sieve (-149 microns) and metal samples to -No. 80 sieve (-177 microns) with an iron mortar and pestle. The slag samples were magnetically cleaned after crushing.

A statistical analysis to determine the standard deviation on the manganese determinations could not be made because of insufficient data.

However, based on prior statistical studies conducted at Homer Research Laboratories, it is estimated that at a 95 percent confidence level the determinations are correct to ±0.02 percent at the 0.20% Mn level and correct to ±0.05 percent at the 4.00% Mn level.

MATHEMATICAL ANALYSIS

The kinetics of heterogeneous reactions necessarily involves the following principal steps:

1. Transport of the reactants from the bulk phases to the interface.
2. Chemical reaction at the interface, which may involve several steps.
3. Transport of the products from the interface into the bulk phase.

If chemical equilibrium is established at the slag-metal interface, the rate of reaction is limited by the rate of diffusion of one or more of the species to or from the interface. Conversely, if differences between concentrations at the interface and bulk concentrations are insignificant, the rate of reaction is determined by the rate of the phase-boundary reaction.

In order to identify the rate-limiting step for manganese oxide reduction from a basic slag by carbon-saturated iron, the reaction was studied at two temperatures and various stirring rates (bubbled CO gas) were used.

In this section, using an approach similar to that employed by Daines[16], theoretical models are derived for four possible diffusion controlling mechanisms. In addition, a rate equation for chemical control

is developed. The mathematical terms used are defined in the nomenclature at the beginning of the thesis. For convenience in data analysis, all the diffusion models are derived in terms of changing manganese concentration in the metal. Then the method employed in making the mathematical computations is discussed in detail.

A. Theoretical Models

1. Diffusion Control

When the rate of a process is controlled by a slow diffusion step, the rate can be defined mathematically by applying Fick's Law, which states that the flux of component i is proportional to the concentration gradient of component i in the direction of diffusion. Stated mathematically

$$J_i = -D_i \frac{dC_i}{dy} \qquad (2)$$

Under most conditions, significant concentration differences are found only in the vicinity of the interface. Therefore, according to Wagner[17], consideration may be confined to the concentration distribution in the boundary layer, and concentration differences in the bulk liquid may be disregarded.

Describing the driving forces in terms of weight percent concentration and the flux in terms of weight percent and interfacial area, Wagner rewrites Equation (2) as:

$$\frac{dC_i}{dt} = \frac{D_i A}{\delta V_{m \text{ or } s}} \cdot [C_i \text{ (interface)} - C_i \text{ (bulk)}] \qquad (3)$$

where the concentration of component i at the interface is that concentation which is in equilibrium with the other components at their instantaneous compositions in the bulk phase.

Wagner's film model, described mathematically by Equation (3), implies the existence of a rigid boundary layer of finite thickness, δ_i. For slag-metal reactions in which turbulent flow conditions exist in the bulk phases, because of carbon monoxide evolution and inductive stirring, the penetration model cited by Tarby and Philbrook[11] seems more appropriate than Wagner's film model. The penetration theory assumes that, for minute elements adjacent to the interface, rigid body motion is maintained for a brief period during which time material is transferred across the interface by unsteady-state diffusion. The thickness of the layer undergoing this flow needs to be sufficiently large, or the contact time sufficiently short, so that diffusion does not penetrate completely through this layer. Thus, the reactants or products are supplied or removed by minute volume elements which are then mixed with the bulk phases and replaced at the interface by new ones. This model requires only that laminar flow conditions exist at the interface, though turbulent flow prevails in the bulk phases.

Describing mass transfer in terms of penetration model, Equation (3) becomes

$$\frac{dC_i}{dt} = \frac{h_i A \rho_{m \text{ or } s}}{W_{m \text{ or } s}} \cdot [C_i \text{ (interface)} - C_i \text{ (bulk)}] \qquad (4)$$

where $V_{m \text{ or } s} = \frac{W_{m \text{ or } s}}{\rho_{m \text{ or } s}}$

Based on Fick's First Law and the penetration model four possible diffusion models are derived below.

a. Diffusion of Manganese in the Metal

If the diffusion of manganese in the metal is the rate-limiting step, the basic rate equation is

$$\frac{d\ \%\ \underline{Mn}}{dt} = \frac{h_{Mn}\ A\ \rho_m}{W_m} \cdot (\%\ \underline{Mn}_i - \%\ \underline{Mn}_b) \qquad (5)$$

At equilibrium, for Equation (1)

$$K = \frac{a_{\underline{Mn}}\ P_{CO}}{a_{(MnO)}\ a_{\underline{C}}} \qquad (6a)$$

The pressure of the carbon monoxide at the interface remained constant at one atmosphere during the experiment. The liquid iron is maintained at carbon saturation in a graphite crucible; hence, the activity of carbon is unity. The experimental data of Schenck and Neumann[26,27] have shown that the activity coefficient of manganese in carbon-saturated iron is best represented by a constant whose value is primarily determined by the carbon content at saturation. Davies, et al[28] have shown the activity coefficient of manganese oxide in the $CaO-Al_2O_3-SiO_2$ system is essentially constant for MnO concentrations up to 8 weight percent. Based on these two studies, it can be assumed that the activity coefficients for manganese and manganese oxide remain constant over the small composition changes experienced during

a run. Therefore, a new equilibrium constant can be defined as

$$K_1 = \frac{\%\ \underline{Mn}_i}{(\%\ MnO)} \tag{6b}$$

Equation (6b) can be rewritten

$$\%\ \underline{Mn}_i = K_1\ (\%\ MnO) \tag{6c}$$

Substituting this in Equation (5), separating variables, and integrating, one obtains

$$\int_{\%\ \underline{Mn}^o}^{\%\ \underline{Mn}^1} \frac{d\ \%\ \underline{Mn}}{K_1\ (\%\ MnO) - \%\ \underline{Mn}} = \frac{h_{Mn}\ A\ \rho_m}{W_m} \cdot (t_1 - t_o) \tag{7}$$

At any time during the run, the concentration of manganese oxide in the slag can be related to that of manganese in the metal by the relationship

$$(\%\ MnO) = (\%\ MnO^o) - Q\ (\%\ \underline{Mn} - \%\ \underline{Mn}^o) \tag{8}$$

When Equation (8) is combined with Equation (7), the only variable under the integral sign is the concentration of manganese in the metal. Integration of the combined expression yields the following rate equation:

$$\frac{-1}{K_1 Q + 1} \cdot \ln \frac{K_1\ \%\ MnO^o + K_1 Q\ \%\ Mn^o - (K_1 Q + 1)\ \%\ Mn^1}{K_1\ \%\ MnO^o - \%\ Mn^o} =$$

$$\frac{h_{Mn}\ A\ \rho_m}{W_m} \cdot (t_1 - t_o) \tag{9}$$

b. Diffusion of Manganese in the Slag

If the diffusion of manganese in the slag is the rate-limiting step, the basic rate equation is

$$- \frac{d\ (\%\ MnO)}{dt} = \frac{h_{MnO}\ A\ \rho_s}{W_s} \cdot [(\%\ MnO_b) - (\%\ MnO_i)] \qquad (10)$$

Expressing Equation (10) in terms of weight percent manganese and going through the same basic arguments used to derive the expression for the diffusion of manganese in the metal, the final rate equation is given as

$$\frac{-K_1 Q}{K_1 Q + 1} \cdot \ln \frac{K_1\ \%\ MnO^o + K_1 Q\ \%\ Mn^o - (K_1 Q + 1)\ \%\ Mn^1}{K_1\ \%\ MnO^o - \%\ Mn^o} =$$

$$\frac{h_{MnO}\ A\ \rho_s}{W_s} \cdot (t_1 - t_o) \qquad (11)$$

c. Diffusion of Oxygen in the Metal

If the diffusion of oxygen in the metal phase is the rate-limiting step, the basic rate equation is

$$\frac{d\ (\%\ \underline{O})}{dt} = \frac{h_o\ A\ \rho_m}{W_m} \cdot (\%\ \underline{O}_i - \%\ \underline{O}_b) \qquad (12)$$

From the known thermodynamic data for the system under consideration, it is estimated that the oxygen concentration at the interface is one or two orders of magnitude larger than the oxygen concentration in the metal.

Therefore, % $\underline{O}_b$ is omitted from Equation (12).

The concentration of oxygen at the interface can be calculated from the standard free energy of reaction for the reaction

$$(MnO) = \underline{Mn} + \underline{O} \tag{13a}$$

For this reaction, at equilibrium, the equilibrium constant is

$$K = \frac{a_{\underline{Mn}}\ a_{\underline{O}}}{a_{(MnO)}} \tag{13b}$$

A review of interaction coefficients found in the Appendix shows that the activity coefficient of oxygen is mainly determined by the carbon content of the metal phase. Relative to the effect of carbon on the activity coefficient of oxygen, the effects of Mn and O are shown to be somewhat inconsequential. Therefore, using the same arguments previously cited, the equilibrium constant can be defined in terms of percent composition at equilibrium as follows:

$$K_2 = \frac{\%\ \underline{Mn}\ \%\ \underline{O}}{(\%\ MnO)} \tag{13c}$$

Equation (13c) can be rewritten

$$\%\ \underline{Mn}_i = K_2\ \frac{(\%\ MnO)}{\%\ \underline{Mn}} \tag{13d}$$

Combining Equations (12) and (13d), expressing weight percent oxygen in terms of weight percent manganese, separating the variables, and integrating,

one obtains the following final rate equation for oxygen diffusion in the metal:

$$\frac{-MW_O}{MW_{Mn} K_2 Q^2} \cdot \left[Q\,(\%\,Mn^1 - \%\,Mn^o) + (\%\,MnO^o + Q\,\%\,Mn^o) \cdot \ln \frac{\%\,MnO^o + Q(\%\,Mn^o - \%\,Mn^1)}{\%\,MnO^o} \right]$$

$$= \frac{h_{\underline{O}}\, A\, \rho_m}{W_m} \cdot (t_1 - t_o) \qquad (14)$$

d. Diffusion of Carbon in the Metal

If diffusion of carbon in the metal phase is the rate-limiting step, the basic rate equation is

$$-\frac{d\,(\%\,\underline{C})}{dt} = \frac{h_{\underline{C}}\, A\, \rho_m}{W_m} \cdot (\%\,\underline{C}_b - \%\,\underline{C}_i) \qquad (15)$$

The concentration of carbon at the interface can be calculated from the standard free energy of the reaction shown as Equation (1). The interaction coefficients found in the Appendix show that the activity coefficient of carbon is mainly determined by the carbon content of the metal phase. With the use of the same arguments used in defining K_1, an equilibrium constant can be defined in terms of percent concentration at equilibrium as follows:

$$K_3 = \frac{\%\,\underline{Mn}}{(\%\,MnO)\,\%\,\underline{O}} \qquad (16a)$$

Equation (16a) can be rewritten

$$\% \underline{C}_i = \frac{\% \underline{Mn}}{K_3 \ (\% MnO)} \tag{16b}$$

The integration of the expression which results from a combination of Equations (15) and (16b) yields the following rate equation for carbon diffusion in the metal:

$$\frac{(MW_C/MW_{Mn})K_3}{K_3 Q \% \underline{C} + 1} \cdot \left[Q(\% Mn^1 - \% Mn^o) - \left(\frac{\% MnO^o + Q \% Mn^o}{K_3 Q \% \underline{C} + 1} \right) \cdot \right. \tag{17}$$

$$\left. \ln \frac{K_3 \% \underline{C} \ (\% MnO^o + Q \% Mn^o) - (K_3 Q \% \underline{C} + 1) \% Mn^1}{K_3 \% \underline{C} \ MnO^o - \% Mn^o} \right] = \frac{h_{\underline{c}} \ A \ \rho_m}{W_m} \cdot (t_1 - t_o)$$

2. Chemical Reaction Control

For a chemically-controlled reaction, the law of mass action states that the rate at which the reaction proceeds is proportional to the activities of the reactants, with each activity raised to a power equal to the number of molecules of each species participating in the reaction. For the reaction under investigation

$$(MnO) + \underline{C} = \underline{Mn} + CO_{(g)} \tag{1}$$

the rate of the reaction in the forward direction is

$$- \frac{dn_{(MnO)}}{dt} = k_1 \ a_{(MnO)} \ a_{\underline{C}} \tag{18}$$

The rate in the reverse direction is

$$\frac{dn_{(MnO)}}{dt} = k_2 \, a_{\underline{Mn}} \, P_{CO} \qquad (19)$$

At any time during the reaction, the net rate of reaction is the sum of Equations (18) and (19)

$$-\frac{dn_{(MnO)}}{dt} = k_1 \, a_{(MnO)} \, a_{\underline{C}} - k_2 \, a_{\underline{Mn}} \, P_{CO} \qquad (20)$$

The pressure of carbon monoxide in the system is one atmosphere. Since the experiments were conducted in a graphite crucible the activity of carbon is unity. Therefore, these terms can be eliminated from Equation (20). Over the range of composition change experienced during a run, it can be assumed that the activity coefficients of manganese and manganese oxide remain constant. Therefore, Equation (20) can be expressed in terms of concentrations as follows

$$-\frac{d\ (\%\ MnO)}{dt} = k_1\ (\%\ MnO) - k_2\ \%\ \underline{Mn} \qquad (21)$$

At equilibrium $\frac{d\ (\%\ MnO)}{dt} = 0$. Hence $K_{eq} = \frac{(\%\ MnO)}{\%\ Mn} = \frac{k_2}{k_1}$

Thus, Equation (21) is rewritten as

$$-\frac{d\ (\%\ MnO)}{dt} = k_1\ [(\%\ MnO) - K_{eq}\ \%\ \underline{Mn}] \qquad (22)$$

Separating the variables and integrating the chemical control rate equation for Equation (1) is

$$\ln \frac{(\%\ MnO) - K_{eq}\ \%\ \underline{Mn}}{(\%\ MnO^{o}) - K_{eq}\ \%\ \underline{Mn}^{o}} = -k\ (t - t_{o}) \qquad (23)$$

$$\text{where } k = k_{1} \frac{(Q + K_{eq})}{Q}$$

B. Treatment of Data

Manganese oxide concentration-time data obtained on the eleven runs made in this study are listed in Table II. The manganese and silicon concentrations in the metal phase at the end of each run are listed in Table III along with operating variables.

The reaction rate equations developed for the reaction under study were derived in terms of manganese concentrations in the metal. Therefore, manganese concentrations in the metal as a function of time were calculated. The calculations were based on the slag manganese-oxide concentrations which had been determined by chemical analysis. A material balance made on the slag-metal system took into account the reduction in slag weight caused by sampling. The slag samples were weighed on all runs except numbers 13 and 15; on these two runs the samples were assumed to weigh 2.0 grams which was the average sample weight obtained on the other heats. Final manganese concentration in the metal phase was used as the starting point for the balance.

Further computations were made on an IBM 360 Model 30 computer using programs written in FORTRAN IV for each of the rate equations. For the four diffusion models the computer was programmed to determine the values for the mass-transfer coefficients (h_i). These values were obtained by integrating from point to point because it was felt the percentage change in slag volume between sampling intervals was significant. For the chemical control rate equation, the computer made a least-squares fit of the data to Equation (23). The slope of this line was equal to the reaction rate constant (k).

The values used for all constants appearing in the four diffusion control rate equations are summarized along with their sources in Table IV. "Calculated" values and the assumptions made in obtaining these values are detailed in the Appendix.

EXPERIMENTAL RESULTS

The thermodynamics and molecularity of the MnO reduction reaction being investigated suggest that the reaction rate, if it is chemically controlled, should be first order reversible (Equation 23). Figure 4 is a plot of Equation 23 using the time-concentration data obtained from Run 24. If the reaction was first order reversible all the data points should fall on a straight line which intersects the origin. From Figure 4, it is obvious the reaction is not a simple first order reversible chemically-controlled reaction. By disregarding the initial data point (the origin) in Figure 4, the data are shown to fall on two distinct straight-lines. Subsequent arguments will show that the reaction occurs in two stages and that the point at which the two "lines" intersect is the division between the two stages.

Figure 4 is typical of the plots obtained from the concentration-time data on all runs except Run 21. The plots differed only in the time at which the intersection occurred and the magnitude of the difference in slope of the two "straight-lines". On all eleven plots the data points in "stage one" were best fit by a curve; however, to facilitate finding the intersection point as previously discussed the initial data points were discarded.

Table V lists the mass-transfer coefficients calculated from Equations (9), (11), (14), and (17). The division between the first and second stage, as determined from the aforementioned plots, is shown by underlining the last value calculated from data falling in stage one. If the reaction were controlled by one of the four proposed diffusion mechanisms, the mass-transfer

coefficients shown in Table V for that model should be of constant value. Clearly, the only reasonable consistency found in Table V is in the values for h_o during the first stage. All the other h values tend to drift with time. In viewing the scatter in stage one h_o values, it must be remembered that the values were calculated using a successive data point technique which is super-sensitive to any errors in the data.

The data points in the second stage were fitted by the least-squares technique to the chemical reaction rate equation for a first order reversible reaction (Equation 23). The fit based on the correlation coefficients, which ranged from 0.9710 to 0.9981, was excellent.

The mass-transfer coefficients, h_o, for the first stage of MnO reduction and the reaction rate constants, k, for the second stage of reduction are grouped by operating parameters in Table VI. Further support for the two stage-two mechanism argument is demonstrated by the consistency of the values within and between the groupings shown in Table VI.

A. Effect of Experimental Parameters on Reaction Rate

A standard technique employed by many investigators to determine whether a heterogeneous reaction is diffusion controlled or chemically controlled is to study the effect of temperature and stirring on the reaction rate. For a chemically-controlled reaction an increase in operating temperature should accelerate the rate of reaction while its effect on a diffusion controlled reaction should be small. In contrast, an increase in stirring rate should have the opposite effect. The effect of bubbling rate, temperature,

and metal phase volume on the rate of MnO reduction are graphically illustrated in Figures 5, 6 and 7. The fact that these variables affected the reaction rate in the prescribed manner is submitted as final proof that the reaction occurs in two stages each of which has a distinct rate-limiting mechanism.

1. Effect of CO Bubbling Rate

Figure 5 shows that the rate of MnO reduction is increased in both stages by increasing the CO bubbling rate. As shown in grouping A of Table VI, both the mass-transfer coefficient, h_o, and the reaction rate constant, k, increase in value as the bubbling rate is increased. This increase in both values is consistent because an increase in bubbling rate not only enhances diffusion via increased stirring, but also increases the effective interfacial area. In comparing the relative increases in h_o and k, it is noted that k shows a larger percentage increase than h_o. Thus, an increase in bubbling rate, was more effective in the second stage (chemically controlled) than in the first stage (diffusion controlled).

Because this observed behavior contradicts the results of the mathematical analysis, it was decided that a qualitative evaluation of the effect of bubbling on mixing within the bath was in order. This was accomplished with a full scale water model of the system. In order to observe the mixing created by bubbling, paper tracers were added to the water. The results of the model study were as follows:

1. When low air flow rates were used, stirring was confined to that portion of the bath in the immediate vicinity of the bubble cone.

2. The eddys created in the bath at low bubbling rates did not result in a continual sweeping of fresh volumes of material to the interface, but rather established a circulation pattern in which the same material was continually swept to and away from the interface.

3. The violent agitation obtained when high air flow rates were employed resulted in a random turbulence pattern in which volumes from every portion of the bath eventually found their way to the interface.

These qualitative observations are supported by observations made in the crucible during the second stage of reduction. At the 50 cc/min. CO bubbling rate, the bubbles broke at the surface in the same localized fashion observed on the model. At the higher flow rate, bubbles were observed breaking over the entire bath surface in a manner similar to that observed on the model during high gas injection rates. The 500 cc/min. flow rate was established as the operating maximum because at higher flow rates material was ejected from the crucible, i.e., the agitation obtained with the 500 cc/min. flow was extremely violent.

The aforementioned observations explain qualitatively the h_o and k values reported in Group A of Table VI. The model showed that the stirring method employed in this study mainly affected the interfacial area. At the 50 cc/min. flow rate, mixing of the type necessary to enhance material transport was negligible. As shown in Group A of Table VI, the value of h_o was

not affected by increasing the bubbling rate from 0 to 50 cc/min. Because of the violent agitation experienced at the 500 cc/min flow rate, mixing of the type necessary to enhance diffusion was experienced; however, the increase in effective interfacial area was still more pronounced than the improvement in mixing.

2. Effect of Temperature

Figure 6 graphically illustrates the effect of temperature on the rate of MnO reduction. In the diffusion-controlled first stage, the time-concentration curves for Runs 20 and 22 parallel each other. That is to say, an increase in temperature had no effect on the reaction rate in this stage. In contrast, in the chemically-controlled second stage an increase in temperature increased the rate of MnO reduction significantly. The increase in value of the reaction rate constants, k, between groupings B and C of Table VI supports the results shown in Figure 6. However, in comparing the h_o values found in Table VI, the values seem to contradict the results shown in Figure 6 for the first stage of reduction. This inconsistency in h_o is attributed to the somewhat questionable accuracy of the thermodynamic coefficients used in calculating K_2, Although the use of an incorrect K_2 value makes it impossible to compare h_o values calculated from data obtained on runs made at different temperatures, it does not destroy the previously cited argument that the consistency of values in and between the groupings in Table VI supports the two stage-two mechanism theory. By simplifying Equation 14 as follows:

$$\frac{-MW_O}{MW_{Mn} K_2 Q^2} \cdot \left[Q\,(\%\,Mn^1 - \%\,Mn^o) + (\%\,MnO^o + Q\,\%\,Mn^o) \cdot \ln \frac{\%\,MnO^1}{\%\,MnO^o} \right]$$

$$= \frac{h_o\, A\, \rho_m}{W_m} \cdot (t_1 - t_o)$$

it is clear that K_2 only affects the magnitude of h_o; it doesn't influence the relative magnitude of h_o values calculated from different pairs of data points within a given heat.

3. Effect of Metal Phase Volume

The volume of the metal phase should have only a minor, perhaps negligible, effect on the rate of reaction. The difference in h_o values found in Table VI for the 285 gm versus the 200 gm heats actually is a result of the difference in turbulence created within the two types of crucibles (see Figure 3) employed in this study. Runs 13 and 15 were made using the larger diameter crucible which contained a raised bottom designed to enhance the flow of heat to the thermocouple. In these runs, the metal charge was set at 270 grams of electrolytic iron to insure an adequate bath depth. Observations made of the bath surface prior to adding the slag to the bath indicated the presence of the raised bottom minimized the inductive stirring effect. It is believed this loss of turbulence in the metal phase explains the low h_o values shown in Table VI for Runs 13 and 15. Because of the bubbler rod design (the gas discharged through a horizontal orifice located

1/2 inch from the rod end) and the presence of the raised crucible bottom, the turbulence created by the CO bubbler was confined to the slag phase.

In Runs 13 and 15 forced stirring of the slag phase and a minimization of stirring in the metal phase resulted in a slower reaction rate in stage one than that experienced in the other runs. This further supports the argument that diffusion in the metal phase is the rate-limiting step in the first stage.

Figure 7 is a plot of the time-concentration curves from Runs 15 and 20. A comparison of the curve slopes shows:

1. The rate of MnO reduction in the first stage is slightly greater in Run 20 where the bubbler was submerged in the metal phase.
2. In stage two, the rate of reduction was slightly greater in Run 20. This slight difference is attributed to the increase in effective interfacial area which resulted from the difference in stirring technique.

4. Effect of Slag Composition

Table I lists the chemical analysis of the two slags employed in this investigation. On trials conducted with Slag No. 1, MnO_2 was blended with the slag before it was added to the crucible. Owing to the instability of MnO_2 under the conditions of these experiments, it was felt that the state of oxidation of manganese was MnO by the time the first slag sample was taken. However, to substantiate this assumption, Run 19 was conducted with Slag No. 2. In Slag No. 2 the MnO was added to the slag as $MnCO_3$ during the

prefusion process. A comparison of the experimental results summarized in Table VI shows that the method of introducing MnO to the slag did not have a discernible effect on the test results. The observed increase in time to the beginning of stage two in Run 19, as compared to the times experienced on the other runs made under the same operating conditions, is explained by the reduction in driving force resulting from the lower initial MnO concentration.

B. Results from Run No. 21

As previously mentioned, the time-concentration data from Run 21 did not fall on two distinct "straight-lines" when a plot of Equation 23 was made. In addition, the h_o values in Table V for Run 21 do not exhibit the consistency found for the other runs. It is thought that the behavior noted in Run 21 is best explained by the lack of temperature control experienced during the run. Normally, bath temperatures were controlled to within ± 5°C of the desired temperature; however, in Run 21 the temperature ranged from 1570°C to 1615°C. The reason for this lack of temperature control cannot be explained.

C. Miscellaneous Reactions

Up to this point, it has been assumed that this kinetic study was made without the interference of other miscellaneous side reactions. The only slag component aside from manganese oxide likely to undergo any appreciable reduction by carbon-saturated iron is silica. As shown in Table III, silica reduction did not occur to any great extent on the eleven runs made. Tarby and Philbrook[11] have shown that the extent of MnO reduction from slag by

reaction with solid graphite is nil. Therefore, it is concluded that the assumption of minimal interference from side reactions is sound.

DISCUSSION

This section is devoted to a comparison of the results of this investigation with the findings of Tarby and Philbrook[11] and Daines[16] for the same reduction reaction.

Tarby and Philbrook's experimental data exhibited exactly the same two-stage behavior found in the kinetic data of this study. Based on the physical appearance of the slag phase, they conclude that stage one is defined by forced convection conditions caused by extensive CO evolution, and that the second stage is defined by natural convection conditions resulting from a subsidence in CO evolution. Using the differential technique of analysis, Tarby and Philbrook found the first stage had an apparent order of reaction greater than unity, while the second stage of reduction behaved as a first-order reaction. Because of the disagreement between the stoichiometry and the order found in stage one, they concluded that the reaction rate must be controlled by a diffusion mechanism. At this point they indicate that the first-order behavior of stage two does not preclude the possibility of diffusion control in that stage. Comparing the magnitude of known diffusion coefficients for transport in liquid iron with diffusion coefficients for transport in slag which are at least an order of magnitude smaller, Tarby and Philbrook conclude that the rate-limiting step in both stages is the diffusion of neutral oxides from the bulk slag to the slag-metal interface.

In comparing Tarby and Philbrook's results with the results of this investigation, complete agreement is found on reaction rate behavior. However,

we disagree on the interpretation of that behavior. To avoid restating the arguments presented in the section on Experimental Results, I will limit my discussion to the following items in Tarby and Philbrook's analysis:

1. The two stages result from a difference in the amount of CO evolved during reaction.
2. Because the diffusion coefficient for MnO transport in slag is smaller than the diffusion coefficients for manganese or oxygen transport in the metal, the rate-limiting step must be diffusion in the slag phase.
3. In accord with the first-order behavior found in the second stage, diffusion is considered to be the rate-limiting mechanism for both stages.

With respect to Item 1, the injection of 500 cc/min. of CO (a volume far surpassing that released by the reaction) did not eliminate the occurrence of two stages. The diffusion coefficient argument is valid only if all the diffusing species have the same driving force (i.e., concentration gradient). There is no justification for such an assumption. Based on the contrasting effect of temperature on the rates of reaction in each of the two stages, Tarby and Philbrook's conclusion (Item 3) is rather questionable.

Daine's analysis is based on reaction rate equations developed for four possible diffusion-limiting steps and three possible chemical rate-controlling mechanisms. Because a good data fit was obtained for all seven models, he attempts to isolate the rate-limiting mechanism by

studying the effects of temperature, stirring rate, melt geometry, and initial MnO concentrations on the reaction rate. Because stirring had no visible effect and temperature had a significant effect on the reaction rate, Daines concludes the reaction is chemically controlled. He then tries to determine which of the three proposed chemical control mechanisms is the rate-limiting step by studying the effects of the slag-to-metal ratio and initial MnO concentrations on the kinetics of the reaction. He points out that neither of these two variables should have any effect on the reaction rate. Finding that this was true for only one of the models, he concludes that that model describes the rate-limiting mechanism (the chemical reaction involving the process of oxygen going from the slag into the metal).

As indicated above, Daines found a reaction rate behavior completely dissimilar from that reported by Tarby and Philbrook and this investigator. Daines' investigation differs from the later two studies in that he employed resistance heating. It has already been pointed out in the section on Experimental Results that inductive stirring had a noticeable effect on the kinetics of the reaction being studied. This raises the interesting and unresolved question of whether we are studying the kinetics of a process rather than the kinetics of a reaction.

Because of the distinct difference in Daines' experimental system and results, my discussion will necessarily be rather limited. It is the opinion of this author that the mechanical stirring employed by Daines would not effectively influence the rate of a reaction known to be controlled by a

diffusion mechanism. The graphite stirring rod employed in his study (a 3/4" diameter graphite rod flattened to 5/8" thickness which was completely submerged in the metal bath) simply will not create the type of mixing needed to continually bring new volumes of material to the reacting interface. In order to achieve the desired type of mixing it is necessary to create an upward or downward component to the flow (as opposed to simple rotation). This could be accomplished by incorporating ribs, spirals, or blades in the stirring rod design. Daines isolates the rate-limiting mechanism by studying the effect of two variables, which he points out should have no effect, on the reaction rate. The arguments based on this rather negative approach seem rather futile.

CONCLUSIONS

The results of the investigation are summarized as follows:

1. The reduction of manganese oxide from $CaO-Al_2O_3-SiO_2$ slag by carbon-saturated iron occurs in two stages.
2. The manner in which MnO is added to the slag does not affect the reaction kinetics.
3. With the use of the unsteady-state penetration theory, the controlling step in the first stage was identified as the transport of oxygen in the metal phase.
4. Reduction in the second stage is described by the rate equation for a chemically-controlled first-order reversible reaction.
5. The contrasting effect of temperature on the rates of reaction in both stages completely supports the two stage-two mechanism analysis determined by the mathematical models.
6. An increase in CO bubbling rate increased the rate of reaction in both stages. Bubbling was found to have a greater effect on the reaction rate in stage two. This inconsistency with respect to the mathematical analysis experienced in reaction rate behavior at different CO bubbling rates is qualitatively explained by observations made on a water model of the system.

TABLE I

A. EXPERIMENTAL MATERIALS

Material	Source	Grade	Quoted % Purity	Form, As Received
Fe	Glidden	Electrolytic	99.9	Fragments
Graphite	Union Carbide	ATJ	94.5	Rods
$CaCO_3$	Fisher Scientific	Reagent	99.4	Powder
SiO_2	Fisher Scientific	Reagent	-	Powder - 140 Mesh
Al_2O_3	Fisher Scientific	Reagent	99.5	Powder
MnO_2	Fisher Scientific	Reagent	99.7	Powder
$MnCO_3$	J. T. Baker Chemical	Reagent	93.5	Powder

B. SLAG ANALYSIS

Slag*	CaO	SiO_2	Al_2O_3	MgO	MnO
1	49.8	39.8	9.9	0.5	-
2	49.5	38.0	8.2	0.1	4.2

* Slag compositions are calculated to 100 percent total. This was done by multiplying the sum of the analyzed values by a factor that would yield 100 percent. The analyzed value for each component was then multiplied by this factor to give the values reported in this table.

TABLE II

EXPERIMENTAL TIME-CONCENTRATION DATA

RUN 13		RUN 15		RUN 16		RUN 17		RUN 18		RUN 19	
t*	%**	t	%	t	%	t	%	t	%	t	%
0	4.43	0	4.16	0	4.53	0	4.50	0	5.16	0	3.52
10	3.18	6	3.03	5	3.65	5	3.27	5	4.10	5	2.62
15	3.02	11	2.63	10	3.33	10	2.77	10	3.44	10	2.27
20	2.76	16	2.33	15	2.94	15	2.42	15	3.13	15	2.11
25	2.53	21	2.13	20	2.85	20	1.90***	20	2.84	20	2.95
30	2.60***	26.33	1.94	25	2.68	25	1.71***	30	2.78	25	1.77
35	2.19	31	1.83	30	2.48	30	1.85	35	2.57	30	1.75
40	2.13	36	1.72	40	2.27	40	1.62	40	2.52	40	1.66
45	2.04	41	1.62	45	2.25	50	1.51	45	2.49	45	1.61
50	1.96	46	1.51	50	2.19	55	1.40	50	2.31	50	1.58
55	1.83	51	1.46	55	2.15	70	1.28	55	2.16	55	1.45
60	1.67	56	1.35	70	1.76			70	1.86	70	1.32
				85	1.65			85	1.78	85	1.25
				115	1.32			100	1.63		

TABLE II (Continued)

RUN 20		RUN 21		RUN 22		RUN 23		RUN 24	
t	%	t	%	t	%	t	%	t	%
0	4.99	0	4.72	0	4.71	0	4.35	0	4.79
5	3.93	5	3.46	5	3.82	5	3.23	5	3.81
10	3.44	10.25	3.12	10	3.33	10	2.77	10	3.44
15	3.10	15	2.93	15	2.93	15	2.42	15	3.07
20	2.87	20	2.57	20	2.81	20	2.29	20	2.84
25	2.67	25	2.49	25	2.74	25	2.06	25	2.73
30	2.48	30	2.17	30	2.61	30	1.91	30	2.55
35	2.34	35	2.12	35	2.44	35	1.89	35	2.44
40	2.20	40	2.07	40	2.27	45	1.47	40	2.38
45	2.02	45	1.80	45	2.23	50	1.46***	45	2.30
50	1.88	50	1.71	50	2.11	55	1.36	50	2.22
55	1.83	55	1.56	55	1.97			55	2.09
70	1.48								
86.5	1.27								

* Time, t, in minutes.
** Concentration of manganese oxide in slag, weight percent.
*** Data points not included in mathematical analysis because of their large deviation from the time-concentration curves.

TABLE III

EXPERIMENTAL PARAMETERS

Run	T, °C	Bubbling Rate cc/Min.	ID of Crucible Inches	Slag Number	Weight, Grams				Final Metal Analysis	
					Fe	C	Slag	MnO_2	% Mn	% Si
13	1500	50	2	1	270	10	95	6	.79	.01
15	1575	50	2	1	270	10	95	6	.95	.04
16	1500	50	1-3/4	1	190	7	95	7	1.23	.04
17	1500	500	1-3/4	1	190	7	95	7	1.33	.12
18	1500	0	1-3/4	1	190	7	95	7	1.30	.04
19	1500	0	1-3/4	2	190	7	100	-	1.11	.08
20	1575	50	1-3/4	1	190	7	95	7	1.54	.20
21	1575	50	1-3/4	1	190	7	95	7	1.41	.23
22	1500	50	1-3/4	1	190	7	95	7	1.15	.03
23	1500	500	1-3/4	1	190	7	95	7	1.38	.09
24	1500	0	1-3/4	1	190	7	95	7	1.27	.04

TABLE IV

MATHEMATICAL CONSTANTS AND VALUES USED IN THEIR DETERMINATION

Term	1500°C	1575°C	Reference
ρ_m	6.78 gm/cc	6.72 gm/cc	18
ρ_s	2.87 gm/cc	2.82 gm/cc	19
γ_{MnO}	.638	.594*	20, 21
%$\underline{C}$	5.15	5.34	21
K_1	5.68	13.7	22
K_2	.0129	.0361	Calculated
K_3	1.03	2.377	Calculated
K_{eq}	.176	.073	22
f_{Mn}	.545	.409	Calculated
$e_c^{(Mn)}$	-.00946	-.01502	Calculated
$\log f_c^{(c)}$	.8166	.8333	23
f_c	6.544	6.613	Calculated
$e_o^{(c)}$	-.32	-.32	24
$e_o^{(o)}$	-.20	-.20	21
f_o	.02259	.01964	Calculated
X_C	.2016	.2078	Calculated
X_{Mn}	% Mn/116.87	% Mn/117.63	Calculated
X_{MnO}	% MnO/120.81	% MnO/120.91	Calculated
% $\underline{O}$	.0065	.0065	25
$\Delta F°$	-	-	21

* Interpolated. Values for γ_{MnO} were available for 1500°C and 1650°C. The value for γ_{MnO} at 1575°C was obtained by assuming the change in γ_{MnO} between 1500°C and 1650°C is linear.

TABLE V

MASS-TRANSFER COEFFICIENTS* CALCULATED FROM EQUATIONS (9), (11), (14), AND (17)

RUN 13				RUN 15				RUN 16			
h_{Mn}	$h_{(MnO)}$	h_o	h_c	h_{Mn}	$h_{(MnO)}$	h_o	h_c	h_{Mn}	$h_{(MnO)}$	h_o	h_c
0.54	9.34	18.71	0.49	0.36	15.13	11.76	0.72	0.91	15.84	36.02	0.90
0.16	2.79	9.10	0.12	0.18	7.67	9.76	0.29	0.39	6.83	26.18	0.33
0.31	5.29	19.20	0.21	0.17	7.07	10.60	0.23	0.52	8.96	42.31	0.39
0.24	4.12	16.61	0.15	0.12	4.92	8.16	0.15	0.12	2.10	11.05	0.08
0.25**	4.27	19.15	0.14	0.12	5.09	9.07	0.14	0.30	5.18	29.00	0.20
0.06**	1.03	4.94	0.03	0.06	2.49	4.64	0.06	0.27	4.75	28.53	0.17
0.12	2.15	10.50	0.06	0.09	3.76	7.23	0.09	0.18	3.06	19.57	0.10
0.13	2.26	11.28	0.06	0.06	2.65	5.24	0.06	0.05	0.93	6.13	0.03
0.21	3.60	18.50	0.09	0.10	4.31	8.77	0.09	0.11	1.89	12.66	0.06
0.23	3.90	20.67	0.10	0.04	1.50	3.13	0.03	0.06	0.97	6.56	0.03
				0.08	3.18	6.70	0.06	0.23	4.01	28.39	0.11
								0.07	1.28	9.45	0.03
								0.13	2.29	17.30	0.05

RUN 17				RUN 18				RUN 19			
1.36	23.52	75.49	1.26	0.98	16.93	34.46	1.09	1.24	21.47	73.16	0.91
0.74	12.79	68.66	0.54	0.76	13.25	57.15	0.69	0.63	10.84	53.15	0.37
0.55	9.51	60.26	0.34	0.39	6.75	37.22	0.31	0.33	5.66	31.07	0.17
0.37	6.33	45.67	0.19	0.39	6.83	42.26	0.28	0.36	6.18	36.09	0.17
0.30	5.12	39.99	0.12	0.04	0.73	4.79	0.03	0.39	6.81	41.98	0.18
0.12	2.15	17.20	0.05	0.31	5.40	36.96	0.20	0.07	1.22	7.71	0.03
0.27	4.71	37.92	0.10	0.09	1.64	11.62	0.06	0.15	2.54	16.44	0.06
0.10	1.73	14.00	0.03	0.05	0.83	5.98	0.03	0.08	1.31	8.58	0.03
				0.03	4.35	31.97	0.15	0.08	1.36	8.94	0.03
				0.27	4.76	36.18	0.15	0.33	5.78	38.56	0.12
				0.18	3.23	25.63	0.09	0.16	2.72	18.59	0.05
				0.05	0.80	6.54	0.02	0.07	1.18	8.16	0.02
				0.10	1.74	14.32	0.04				

Table V (Continued)

RUN 20				RUN 21***				RUN 22			
h_{Mn}	$h_{(MnO)}$	h_o	h_c	h_{Mn}	$h_{(MnO)}$	h_o	h_c	h_{Mn}	$h_{(MnO)}$	h_o	h_c
0.41	17.32	19.53	1.03	0.56	23.47	31.88	1.27	0.88	15.22	40.09	0.90
0.25	10.34	19.19	0.50	0.18	7.55	15.89	0.33	0.58	10.05	44.21	0.50
0.19	8.00	18.05	0.35	0.12	4.90	11.52	0.20	0.56	9.73	53.56	0.42
0.13	5.40	13.56	0.21	0.23	9.58	24.87	0.35	0.16	2.84	17.36	0.11
0.12	5.11	13.78	0.19	0.06	2.41	6.72	0.08	0.09	1.47	9.27	0.06
0.13	5.54	15.86	0.19	0.23	9.65	28.49	0.30	0.18	3.07	19.89	0.11
0.08	3.37	10.08	0.11	0.02	0.95	2.94	0.03	0.29	4.95	33.49	0.17
0.11	4.52	13.98	0.14	0.05	1.97	6.13	0.05	0.26	4.44	31.44	0.15
0.14	5.86	18.85	0.16	0.23	9.68	31.25	0.25	0.05	0.94	6.77	0.03
0.10	4.32	14.05	0.11	0.06	2.36	7.88	0.06	0.23	3.92	28.90	0.11
0.05	2.25	7.60	0.06	0.15	6.44	21.99	0.14	0.24	4.20	31.75	0.12
0.10	4.21	14.73	0.09								
0.08	3.34	12.13	0.06								

RUN 23				RUN 24			
1.22	21.16	91.41	1.11	0.98	17.04	60.89	1.01
0.59	10.17	62.00	0.43	0.41	7.17	37.74	0.36
0.56	9.62	66.56	0.35	0.51	8.76	53.88	0.40
0.21	3.57	26.25	0.12	0.32	5.55	38.00	0.23
0.39	6.84	52.29	0.21	0.17	2.97	21.41	0.12
0.32	5.47	43.29	0.15	0.27	4.73	35.47	0.17
0.07	1.15	9.27	0.03	0.19	3.38	26.23	0.12
0.46	8.03	66.41	0.19	0.10	1.75	13.91	0.06
0.14	2.47	20.72	0.05	0.10	1.81	14.51	0.06
				0.16	2.84	23.18	0.09
				0.23	3.99	33.24	0.12

* cm/sec x 10^4
** Division between Stage 1 and Stage 2.
*** Division between Stages 1 and 2 not apparent.

TABLE VI

SUMMARY OF THE MASS TRANSFER COEFFICIENTS FOR THE FIRST STAGE AND THE REACTION RATE CONSTANTS FOR THE SECOND STAGE OF MnO REDUCTION

A. 1500°C, 200 gms Metal

Run No.	Bubbling Rate CO, cc/min.	Average h_o^* cm/sec x 10^4	k, min^{-1} x 10^3	Time to Start of Second Stage, min.
18	0	42.77	8.83	20
19	0	47.09	7.71	25
24	0	47.63	9.67	20
16	50	34.84	9.36	15
22	50	45.95	11.39	15
17	500	68.14	13.81	15
23	500	73.32	18.12	15

B. 1500°C, 50 cc/min. CO

Run No.	Metal, gms	Average h_o cm/sec x 10^4	k, min^{-1} x 10^3	Time to Start of Second Stage, min.
13	285	16.55	11.77	35
16	200	34.84	9.36	15
22	200	45.95	11.39	15

C. 1575°C, 50 cc/min. CO

Run No.	Metal, gms	Average h_o cm/sec x 10^4	k, min^{-1} x 10^3	Time to Start of Second Stage, min.
15	285	9.87	12.66	26.33
20	200	18.92	13.63	15

* An average of the h_o values appearing in Table V for the first stage of reduction.

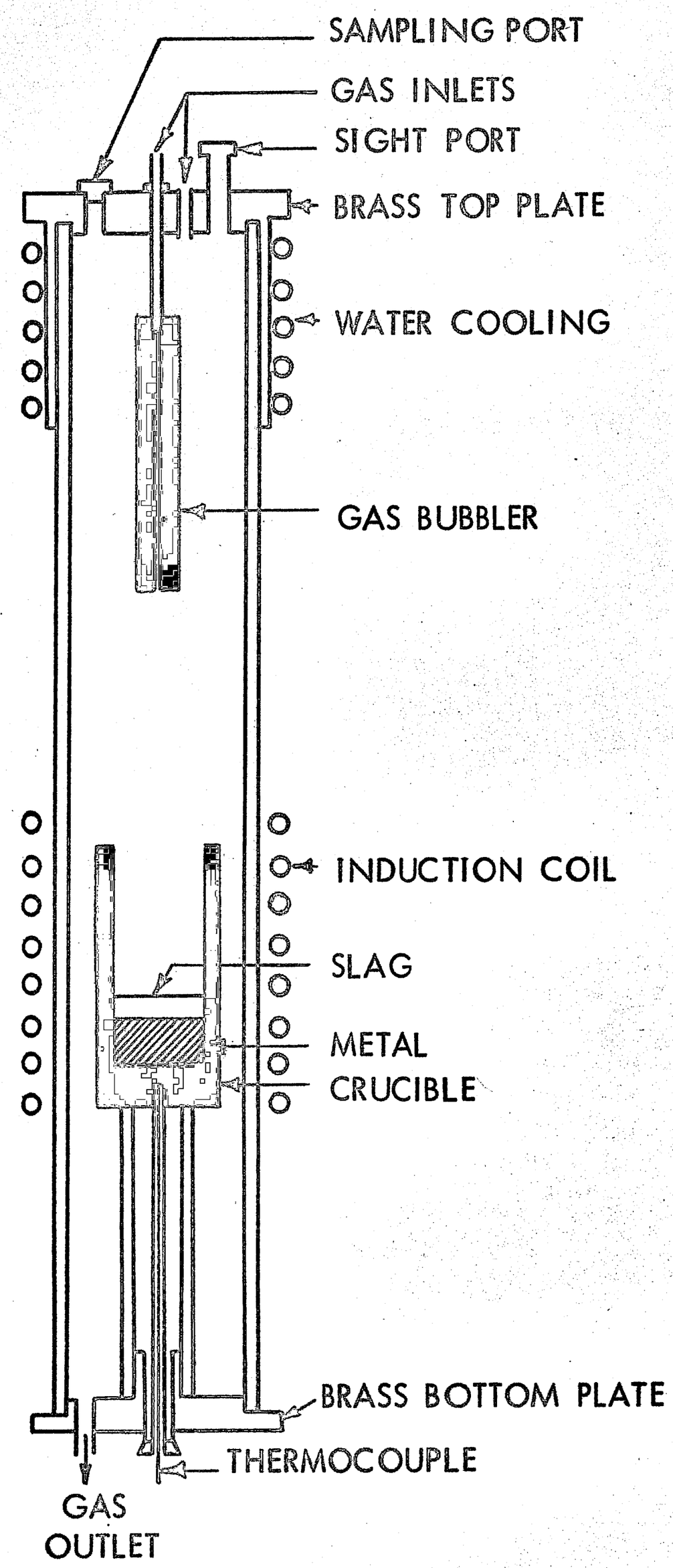

FIGURE 1. INDUCTION TUBE FURNACE ASSEMBLY

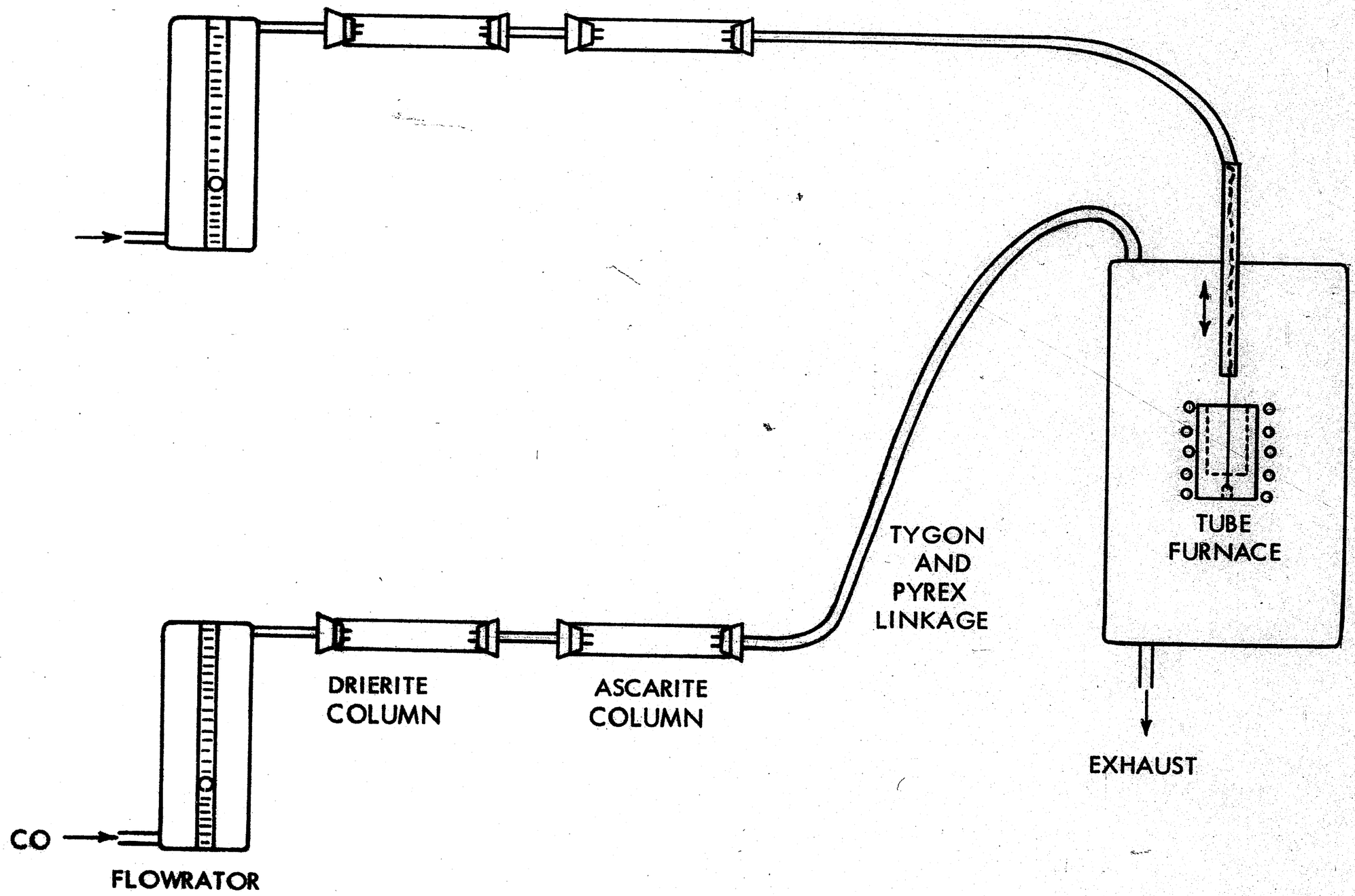

FIGURE 2. DIAGRAM OF GAS PURIFYING TRAIN

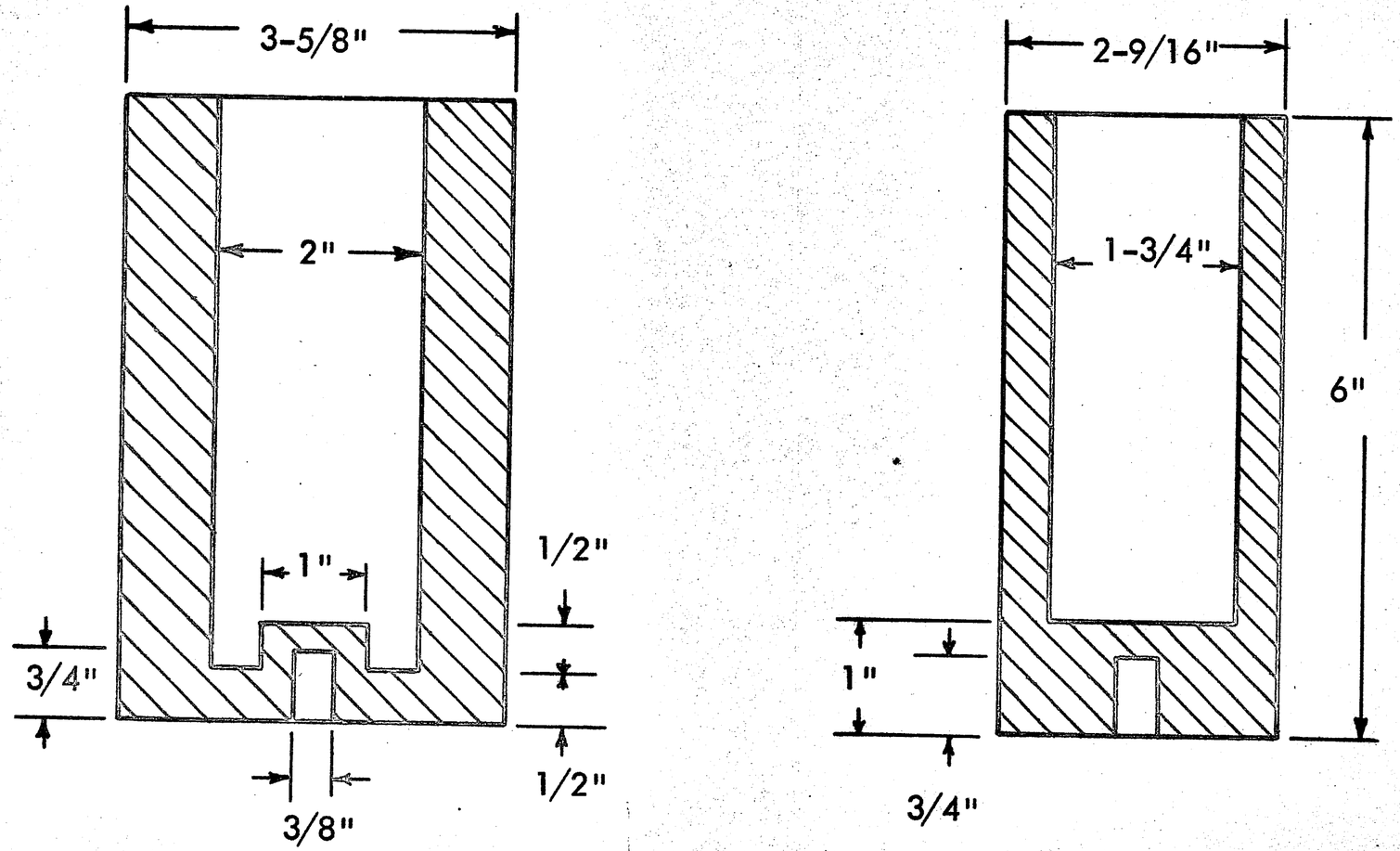

FIGURE 3. SECTIONAL VIEW OF GRAPHITE CRUCIBLES

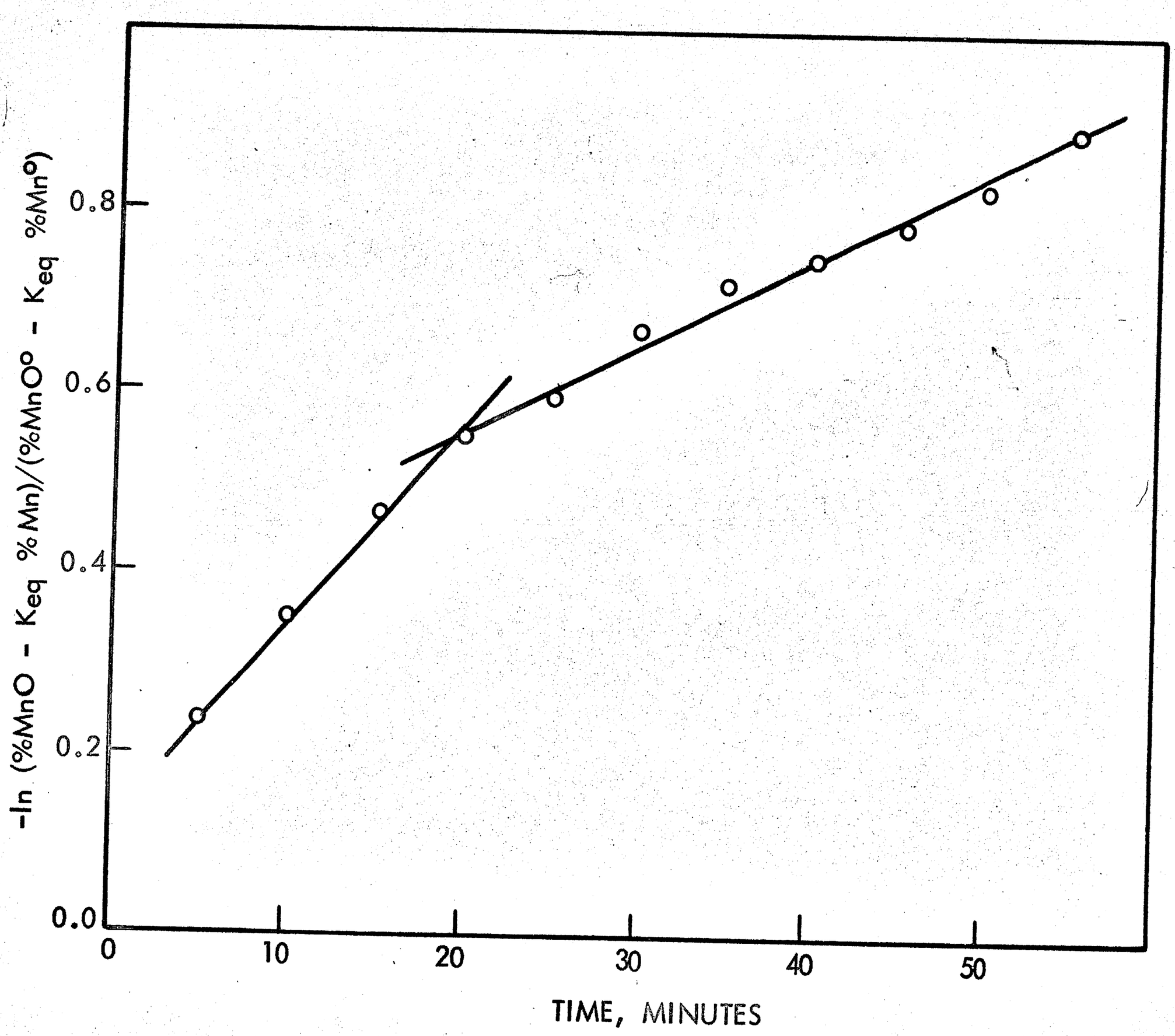

FIGURE 4. PLOT OF $-\ln (\%MnO - K_{eq}\ \%Mn)/(\%MnO^{o} - K_{eq}\ \%Mn^{o})$ VS TIME, RUN 24

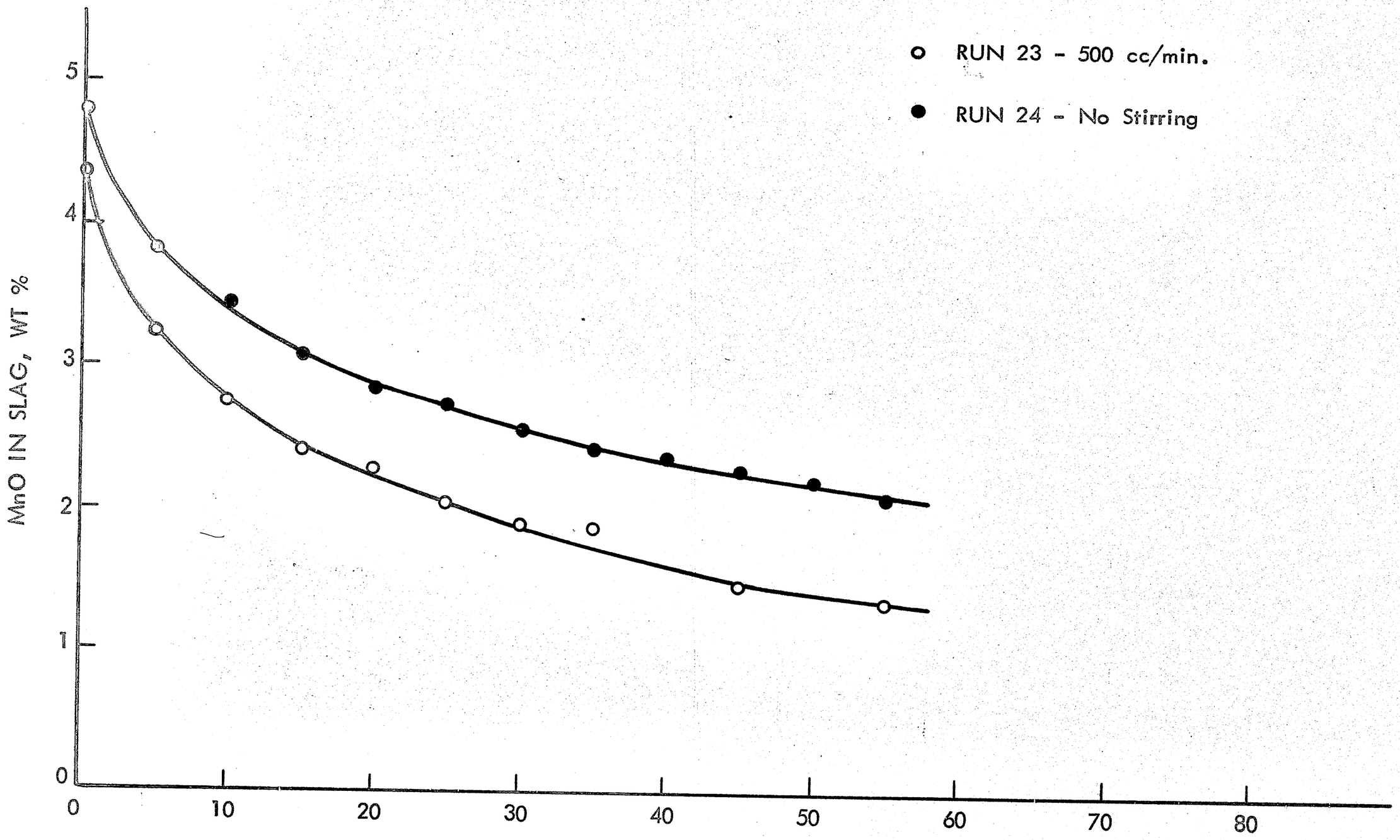

FIGURE 5. MnO CONCENTRATION VS TIME, 1500°C, 200 gms METAL

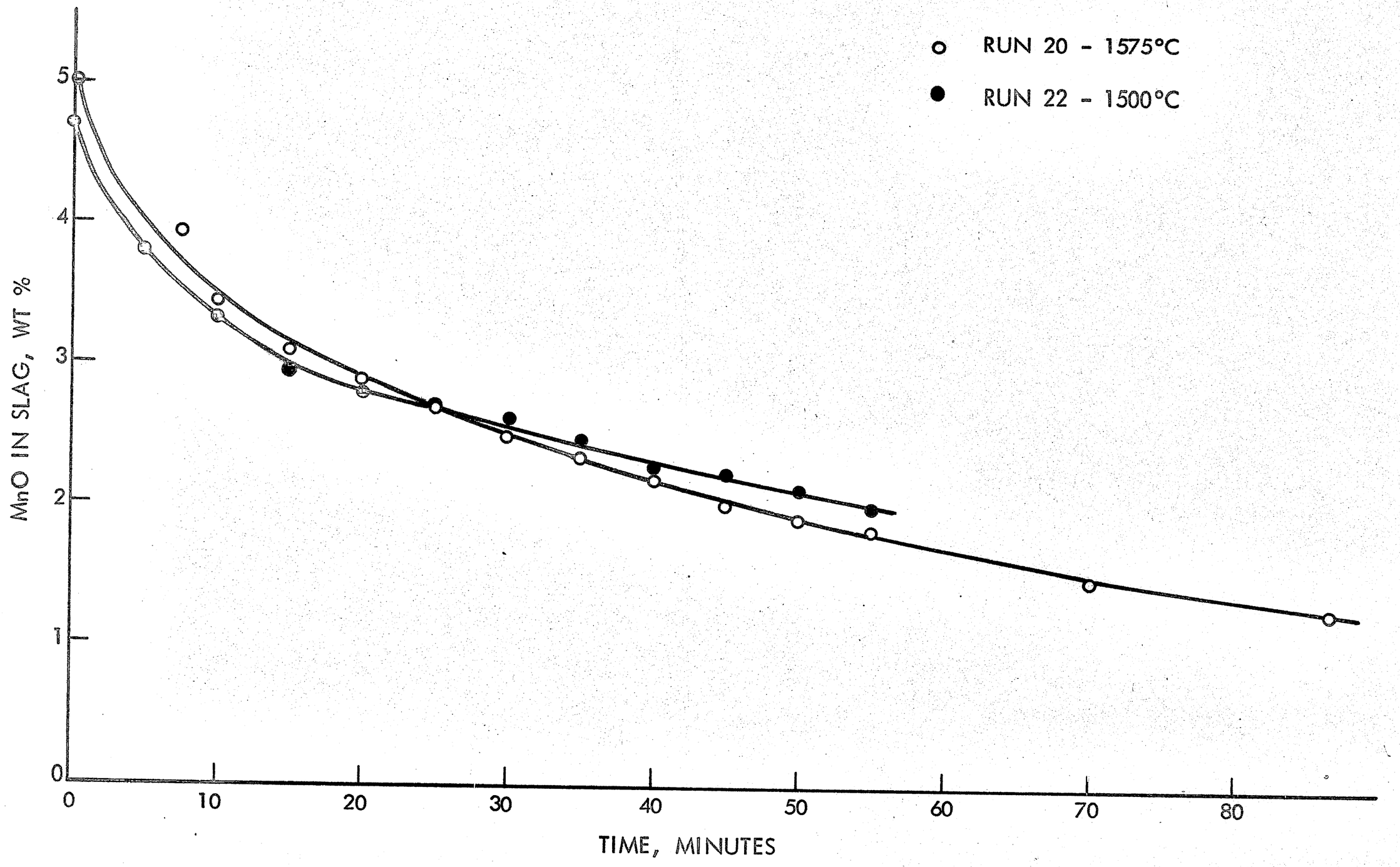

FIGURE 6. MnO CONCENTRATION VS TIME, 50 cc/min. CO, 200 gms METAL

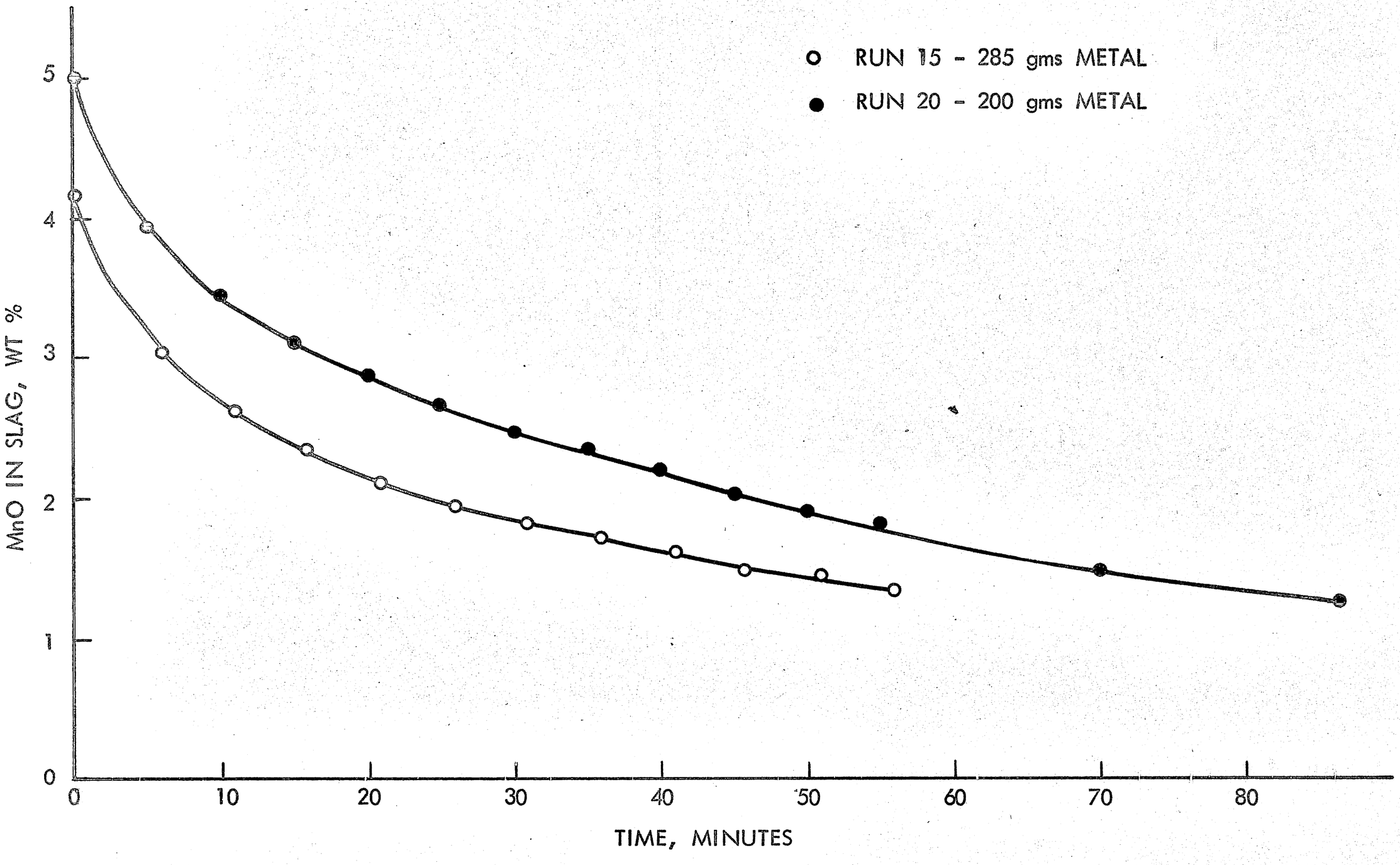

FIGURE 7. MnO CONCENTRATION VS TIME, 1575°C, 50 cc/min. CO

APPENDIX

CALCULATION OF THE CONSTANTS APPEARING IN THE DIFFUSION MODELS

A. Calculation of Mole Fractions - X_C, X_{Mn}, X_{MnO}.

The average % Mn and % MnO for all runs was determined as follows:

$$\%Mn_{ave} = \frac{\Sigma(\%\ Mn^f - \%\ Mn^o)/2}{n^*} = .74\%\ Mn\ @\ 1500°C,\ .86\%\ Mn\ @\ 1575°C$$

$$\%\ MnO_{ave} = \frac{\Sigma(\%\ MnO^f - \%\ MnO^o)/2}{n^*} = 3.02\%\ MnO\ @\ 1500°C,\ 3.13\%\ MnO\ @\ 1575°C$$

These values were then used in determining the mole fraction of carbon, manganese, and manganese oxide as follows:

$$X_C = \frac{\%\ C/MW_C}{\frac{\%\ Fe}{MW_{Fe}} + \frac{\%\ Mn_{ave}}{MW_{Mn}} + \frac{\%\ C}{MW_C}} = .2016\ @\ 1500°C,\ .2078\ @\ 1575°C$$

where $\%\ Fe + \%\ C + \%\ Mn_{ave} = 100.0$

$$X_{Mn} = \frac{\%\ Mn}{MW_{Mn}\left(\frac{\%\ Fe}{MW_{Fe}} + \frac{\%\ C}{MW_C} + \frac{\%\ Mn_{ave}}{MW_{Mn}}\right)} = \frac{\%\ Mn}{116.87}\ @\ 1500°C,\ \frac{\%\ Mn}{117.53}\ @\ 1575°C$$

$$X_{MnO} = \frac{\%\ MnO}{MW_{MnO}\left(\frac{\%\ CaO}{MW_{CaO}} + \frac{\%\ SiO_2}{MW_{SiO_2}} + \frac{\%\ Al_2O_3}{MW_{Al_2O_3}} + \frac{\%\ MgO}{MW_{MgO}} + \frac{\%\ MnO_{ave}}{MW_{MnO}}\right)}.$$

$$X_{MnO} = \frac{\%\ MnO}{120.81}\ @\ 1500°C,\ \frac{\%\ MnO}{120.91}\ @\ 1575°C$$

n^* is the number of runs made at 1500°C and 1575°C respectively.

B. Calculation of Interaction Coefficient - $e_c^{(Mn)}$.

$$Mn + CO = MnO \text{ (1 in FeO)} + C$$

$$\Delta F^o = -58,150 + 36.35T = -RT \ln K$$

$K = .1673$ @ 1500°C, .0856 @ 1575°C

$$K = \frac{a_{MnO}}{a_{Mn}} = \frac{\gamma_{MnO}\ X_{MnO}}{\gamma_{Mn}\ X_{Mn}}$$

$$K_{1500°C} = .1673 = \frac{.638\ \frac{\%\ MnO}{120.81}}{\gamma_{Mn}\ \frac{\%\ Mn}{116.87}}$$

From Philbrook and Tarby[22],

$$\left(\frac{\%\ MnO}{\%\ Mn}\right)_{1500°C} = .176$$

$$\gamma_{Mn}{}_{1500°C} = \frac{.638\ (.176)\ (116.87)}{.1673\ (120.81)} = .649$$

Similarly, $\gamma_{Mn}{}_{1575°C} = .493$

The only element affecting the activity coefficient of manganese in the system being studied is carbon. Therefore,

$$\gamma_{Mn} = \gamma_{Mn}^{(c)}$$

$$@\ 1500°C\ \ln \gamma_{Mn}^{(c)} = -.43232 = \varepsilon_{Mn}^{(c)}\ X_C$$

$$\varepsilon_{Mn}^{(c)} = \frac{.43232}{.2016} = -2.144 = \varepsilon_{Mn}^{(c)}$$

$$e_c^{(Mn)} = \frac{0.2425}{54.94}\ \varepsilon_c^{(Mn)} = \underline{-.00946}$$

similar, @ 1575°C

$$\varepsilon_{Mn}^{(c)} = -3.403$$

$$e_{c}^{(Mn)} = \underline{-.01504}$$

C. Calculation of the Henrian Activity Coefficient of Manganese - f_{Mn}.

$$\%\ \underline{Mn} + CO = (MnO) + C$$

$$\Delta F^{o} = -58,150 + 45.46T = -RT \ln K$$

$$K = 1.708 \times 10^{-3} \text{ @ } 1500°C,\ 8.76 \times 10^{-4} \text{ @ } 1575°C$$

$$K = \frac{a_{MnO}}{f_{Mn}\ \%\ Mn} = \frac{\gamma_{MnO}\ X_{MnO}}{f_{Mn}\ \%\ Mn}$$

$$f_{Mn_{1500°C}} = \frac{.638\ (.176)}{120.81\ (1.703 \times 10^{-3})} = .545$$

similarly, $f_{Mn_{1575°C}} = .409$

D. Calculation of the Henrian Activity Coefficient of Carbon - f_{c}.

$$\log f_{c} = \log f_{c}^{(c)} + \log f_{c}^{(Mn)}$$

$$\log f_{c} = \log f_{c}^{(c)} + e_{c}^{(Mn)}\ \%\ Mn_{ave}$$

$$\log f_{c_{1500°C}} = .8166 + (-.00946)\ (.74) = 0.8159$$

$$f_{c_{1500°C}} = 6.544$$

$$\log f_{c_{1575°C}} = .8333 + (-.01502)\ (.86) = 0.8204$$

$$f_{c_{1575°C}} = 6.613$$

E. Calculation of the Henrian Activity Coefficient of Oxygen - f_o.

$$\log f_o = e_o^{(c)}\ \%\ \underline{C} + e_o^{(o)}\ \%\ \underline{O} + e_o^{(Mn)}\ \%\ \underline{Mn}$$

$$\log f_o = -.32\%\ \underline{C} - .20\%\ \underline{O} + 0.0\ \%\ \underline{Mn}$$

$$\log f_{o_{1500°C}} = -.32\ (5.15) - .20\ (.0065) = -1.64813$$

$$f_{o_{1500°C}} = .02259$$

$$\log f_{o_{1575°C}} = -.32\ (5.34) - .20\ (.0065) = -1.70893$$

$$f_{o_{1575°C}} = .01964$$

Specific values for $e_o^{(c)}$ and $e_o^{(o)}$ at 1500°C and 1575°C were not available; however, these values were reported to be acceptable in this temperature range.

F. Evaluation of the Equilibrium Constant - K_2.

$$(MnO) = \underline{\%\ Mn} + \underline{\%\ O}$$

$$\Delta F^o = 58{,}400 - 25.98T = -RT \ln K$$

$$K = .0301 \text{ @ } 1500°C,\ .05905 \text{ @ } 1575°C$$

$$K = \frac{f_{Mn}\ \%\ \underline{Mn}\ f_o\ \%\ \underline{O}}{\gamma_{MnO}\ X_{MnO}}$$

$$K_{2_{1500°C}} = \frac{\%\ \underline{Mn}\ \%\ \underline{O}}{\%\ MnO} = \frac{K\ \gamma_{MnO}}{f_{Mn}\ f_o\ (120.81)}$$

$$K_{2_{1500°C}} = \frac{.0301\ (.638)}{(.545)\ (.02259)\ (120.81)} = .0129$$

$$K_{2_{1575°C}} = \frac{.05905\ (.594)}{(.409)\ (.01964)\ (120.91)} = .0361$$

G. Evaluation of the Equilibrium Constant - K_3.

$$(MnO) + \%\ \underline{C} = \%\ \underline{Mn} + CO$$

$$\Delta F^o = 53{,}050 - 35.46T = -RT \ln K$$

K = 16.24 @ 1500°C, 29.93 @ 1575°C

$$K = \frac{f_{Mn}\ \%\ \underline{Mn}}{\gamma_{MnO}\ X_{MnO}\ f_c\ \%\ C}$$

$$K_{3_{1500°C}} = \frac{\%\ Mn}{\%\ MnO\ \%\ C} = \frac{K\ \gamma_{MnO}\ f_c}{f_{Mn}\ (120.81)}$$

$$K_{3_{1500°C}} = \frac{16.24\ (.638)\ (6.544)}{.545\ (120.31)} = 1.03$$

$$K_{3_{1575°C}} = \frac{29.93\ (.594)\ (6.613)}{.409\ (120.91)} = 2.377$$

REFERENCES

1. L. Chang and K. M. Goldman, "Kinetics of the Transfer of Sulfur Across a Slag-Metal Interface," Trans. AIME, 176, 309 (1949).

2. N. J. Grant, U. Kalling, and J. Chipman, "Effects of Manganese and Its Oxide on Desulphurization by Blast-Furnace Type Slags," Trans. AIME, 191, 666 (1951).

3. N. J. Grant, O. Troili, and J. Chipman, "The Effect of Silica Reduction on Blast Furnace Desulfurization," Trans. AIME, 191, 672 (1951).

4. G. Derge, W. O. Philbrook, and K. M. Goldman, "Effect of Si, Mn, P, Al, C, Ni, and Cu on the Mechanism of Sulfur Transfer Across a Slag-Metal Interface," Trans. AIME, 200, 534 (1954).

5. H. P. Schulz, "Fundamentals of Sulfur Reactions. I. Equilibria. II. Kinetics," Arch. Eisenhuettenw, 35, 803 (1964).

6. S. Ramachandran, T. B. King, and N. J. Grant, "Rate and Mechanism of the Sulfur Transfer Reactions," Trans. AIME, 206, 1549 (1956).

7. T. B. King and S. Ramachandran, "Electrochemical Nature of Sulfur Transfer in the System Carbon-Saturated-Iron-Slag," The Physical Chemistry of Steelmaking, Wiley and Sons, New York, 1958, pp. 125-135.

8. J. Chipman and J. C. Fulton, "Kinetic Factors in the Desulfurization of Pig Iron by Blast-Furnace Type Slags," The Physical Chemistry of Steelmaking, Wiley and Sons, New York, 1958, pp. 113-116.

9. T. E. Dancy, "The Kinetics of the Reduction of Iron Oxide Above 1400°C," Jnl. Iron and Steel Inst., 169, 17 (1951).

10. W. O. Philbrook and L. D. Kirkbride, "Rate of FeO Reduction from a CaO-SiO_2-Al_2O_3 Slag by Carbon-Saturated Iron," Trans. AIME, 206, 351 (1956).

11. S. K. Tarby and W. O. Philbrook, "The Rate and Mechanism of the Reduction of FeO and MnO from Silicate and Aluminate Slags by Carbon-Saturated Iron," Trans. TMS-AIME, 239, 1005 (1967).

12. C. W. McCoy and W. O. Philbrook, "Slag-Metal Reactions of Chromium in Carbon-Saturaterated Melts," The Physical Chemistry of Steelmaking, Wiley and Sons, New York, 1958, pp. 93-98.

13. J. Chipman and J. C. Fulton, "Kinetic Factors in the Reduction of Silica from Blast-Furnace Type Slags," Trans. TMS-AIME, 215, 888 (1959).

14. J. R. Rawling and J. F. Elliott, "The Reduction of Silica in Blast Furnace Slag-Metal Systems," Trans. TMS-AIME, 233, 1539 (1965).

15. E. T. Turkdogan, P. Grieveson, and J. F. Beisler, "Kinetics and Equilibrium Considerations for Silicon Reaction Between Silicate Melts and Graphite-Saturated Iron. Part II: Reaction Kinetics of Silica Reduction," Trans. TMS-AIME, 227, 1265 (1963).

16. W. L. Daines, "Kinetics of Manganese Oxide Reduction from Basic Slags by Silicon and Carbon Dissolved in Liquid Iron," Ph. D. Thesis, The University of Michigan, 1966.

17. C. Wagner, "Kinetic Problems in Steelmaking," The Physical Chemistry of Steelmaking, Wiley and Sons, New York, 1958, pp. 237-251.

18. L. D. Lucas, "Density of Iron-Carbon Mixtures in the Liquid State," COMPTE, rend., 248, pp. 2336-38, (1959).

19. L. R. Barrett and A. G. Thomas, "Surface Tension and Density Measurements on Molten Glasses in the $CaO-Al_2O_3-SiO_2$ System," J. Soc. Glass Technol., 43 [211], pp. 179-90T, (1959).

20. H. Schenck and F. Neumann: Arch. Eisenhuttenw., 31, pp. 83-86, (1960).

21. J. F. Elliott, M. Gleiser, and V. Ramakrishna, Thermochemistry for Steelmaking, Vol. II, Addison-Wesley Publishing Co., Reading, Mass., 1963.

22. W. O. Philbrook and S. K. Tarby, "Distribution of Manganese Between Silicate and Aluminate Slags and Carbon - Saturated Iron," Trans. TMS-AIME, 227, 1039, (1963).

23. A. Rist and J. Chipman, "Activity of Carbon in Liquid Iron-Carbon Solutions," The Physical Chemistry of Steelmaking, Wiley and Sons, New York, 1958, pp. 3-12.

24. S. Banya and S. Matoba, Technol. Rep. Tahoku Univ., Sendai, 22, pp. 97-108, (1957).

25. J. F. Elliott, "The Carbon-Oxygen Equilibria in Liquid Iron," The Physical Chemistry of Steelmaking, Wiley and Sons, New York, 1958, pp. 37-41.

26. H. Schenck and F. Neuman, "Reaction Equilibria of Manganese and Silicon between Molten Carbon-Saturated Iron Heats and Lime-Silicon Slags at 1450° to 1550°," Arch. Eisenhuttenw, 30, 705 (1959).

27. H. Schenck and F. Neuman, "The Effect of Magnesium and Aluminum Oxides on Manganese Reaction Equilibria between Silicon-containing Iron, saturated with Carbon, and Limestone-Silica Slags at 1500°C," Arch. Eisenhuttenw, 31, 83 (1960).

28. M. W. Davies, K. P. Abraham, and F. D. Richardson, "Activities of Manganese Oxide in Silicate Melts," Jnl. Iron and Steel Inst., 196, 82, (1960).

VITA

David Mathias Koncsics was born on October 19, 1938 in Allentown, Pennsylvania. His parents are Mathias Koncsics and Dorothy M. (Krasely). After graduating from Allen High School in Allentown, Pennsylvania in June of 1956, he entered the Pennsylvania State University. He received the Degree of Bachelor of Science in Metallurgy in June of 1960. From July 1960 until June 1963 he was employed by the Open Hearth Division of the Bethlehem Steel Corporation in Sparrows Point, Maryland. Mr. Koncsics worked on the development of an Open Hearth Oxygen Lance Practice. In July of 1963, Mr. Koncsics was transferred to the Steelmaking Section of the Homer Research Laboratories, Bethlehem Steel Corporation, Bethlehem, Pennsylvania. Presently Mr. Koncsics is working on the Continuous Casting Process.

He is married to the former Jean Phyllis Baret of Pittsburgh, Pennsylvania and has three children.